ISSN 1028-334X, Doklady Earth Sciences, 2006, Vol. 411A, No. 9, pp. 1389–1392. © Pleiades Publishing, Inc., 2006.
Original Russian Text © M.Yu. Koreshkova, L.P. Nikitina, N.V. Vladykin, D.I. Matukov, 2006, published in Doklady Akademii Nauk, 2006, Vol. 411, No. 3, pp. 370–374.

GEOCHEMISTRY

U–Pb Dating of Zircon from the Lower Crustal Xenoliths, Udachnaya Pipe, Yakutia

M. Yu. Koreshkova[a], L. P. Nikitina[b], N. V. Vladykin[c], and D. I. Matukov[d]

Presented by Academician I.D. Ryabchikov, December 28, 2005

Received January 17, 2006

DOI: 10.1134/S1028334X06090121

Issues of the origin and age of lower crustal xenoliths from kimberlites of the Siberian Craton are considered in [1–5]. The Grt–Cpx Sm–Nd isotope age of granulite from the Udachnaya Pipe is 1756 Ma [1]. Model ages of xenoliths in pipes of the Anabar Block correspond to the Archean [5].

This paper presents results of zircon dating of xenoliths from the Udachnaya Pipe. Mafic two-pyroxene garnet granulites (samples uk1 and uk2), mafic amphibole-bearing garnet granulite (uk11), and intermediate garnet granulite (uk5) were taken for age determination. The mafic two-pyroxene garnet granulites correspond to tholeiitic basalts. Xenolith uk1 shows differentiated REE distribution ($La_n/Yb_n = 3.9$); depletion in Ti, Nb, and other HFSE; and enrichment in LILE, including Pb, which is typical of island-arc tholeiites. Sample uk 21 has a flat PM-normalized REE pattern with an insignificant Nb maximum and Pb minimum. Its protoliths was presumably ocean floor basalt. Xenolith uk11 differs from other xenoliths in the high content of incompatible elements, which can be related to contamination by host kimberlites or metasomatism. Granulite uk5 is characterized by elevated contents of Al_2O_3 and alkalis, as well as a fractionated REE pattern with LREE enrichment, HREE depletion, and Eu maximum (Eu/Eu* = 1.32). This geochemistry suggests a monzonitic composition of the protolith.

[a] *St. Petersburg State University, Universitetskaya nab. 7/9, St. Petersburg, 199164 Russia; e-mail: marina@mk3909.spb.edu*

[b] *Institute of Precambrian Geology and Geochronology, Russian Academy of Sciences, nab. Makarova 2, St. Petersburg, 199034 Russia*

[c] *Vinogradov Institute of Geochemistry and Analytical Chemistry, Siberian Division, Russian Academy of Sciences, ul. Favorskogo 1a, Irkutsk, 664033 Russia*

[d] *Center of Isotopic Studies, Karpinskii All-Russia Research Institute of Geology, Srednii pr. 74, St. Petersburg, 199106 Russia*

The equilibrium temperature and pressure of the granulite assemblage are within 720–810°C and 0.9–1 GPa. They were calculated for grain cores using Grt–Cpx geothermometers [9, 10], a Grt–Cpx–Pl–Qz geobarometer [11], and a Grt–Opx thermobarometer [12].

Zircon grains were hand picked under binocular microscope and were cast in an epoxy mount together with standard zircon grains TEMORA and 91 500. To choose analytical spots, we used optical and cathodoluminescence images. The U–Pb dating was conducted on a SHRIMP II ion microprobe at the Center of Isotopic Studies of Karpinskii All-Russia Institute following technique [6]. The intensity of the primary beam of negative molecular oxygen ions was 4 nA, and the Spot (crater) diameter was 18 μm. The data obtained were treated with SQUID software [7]. The U–Pb ratios were normalized to 0.0668 in TEMORA standard zircon corresponding to an age of 416.75 Ma [8]. Uncertainties of individual analyses (ratios and age values) are given at the 1σ level; uncertainties of calculated age values, at the 2σ level.

Zircon forms short-prismatic or oval grains 100–200 μm in size. The cathodoluminescence images demonstrate dark cores with thin rhythmic zoning and light rims (Fig. 1). Grains from one sample have a similar internal structure. Zircon from xenolith uk1 has thin and homogeneous rims (Figs. 1a, 1b). Zircons from samples uk21 and uk5 have thick concentric-zonal rims (Figs. 1c, 1d). Thick rims of grains in sample uk11 demonstrate a chaotic structure (Figs. 1e, 1f; the grain in Fig. 1f lacks a zoned core). Cores are rounded or angular, occasionally crosscut by fractures and cemented by light "zircon," but fragments of cores are not displaced from each other (Fig. 1b).

Rims yield concordant ages, which are identical within the error limits in all samples. Rims in xenolith uk1 have an age of 1824 ± 20 Ma (MSWD = 0.69), while sample uk5 has an age of 1827 ± 14 Ma (MSWD = 2.4). In samples uk11 and uk21, rims and cores have virtually identical ages (table). Concordant values (on two points in each sample) are 1831 ± 16 Ma (MSWD = 1.8) for

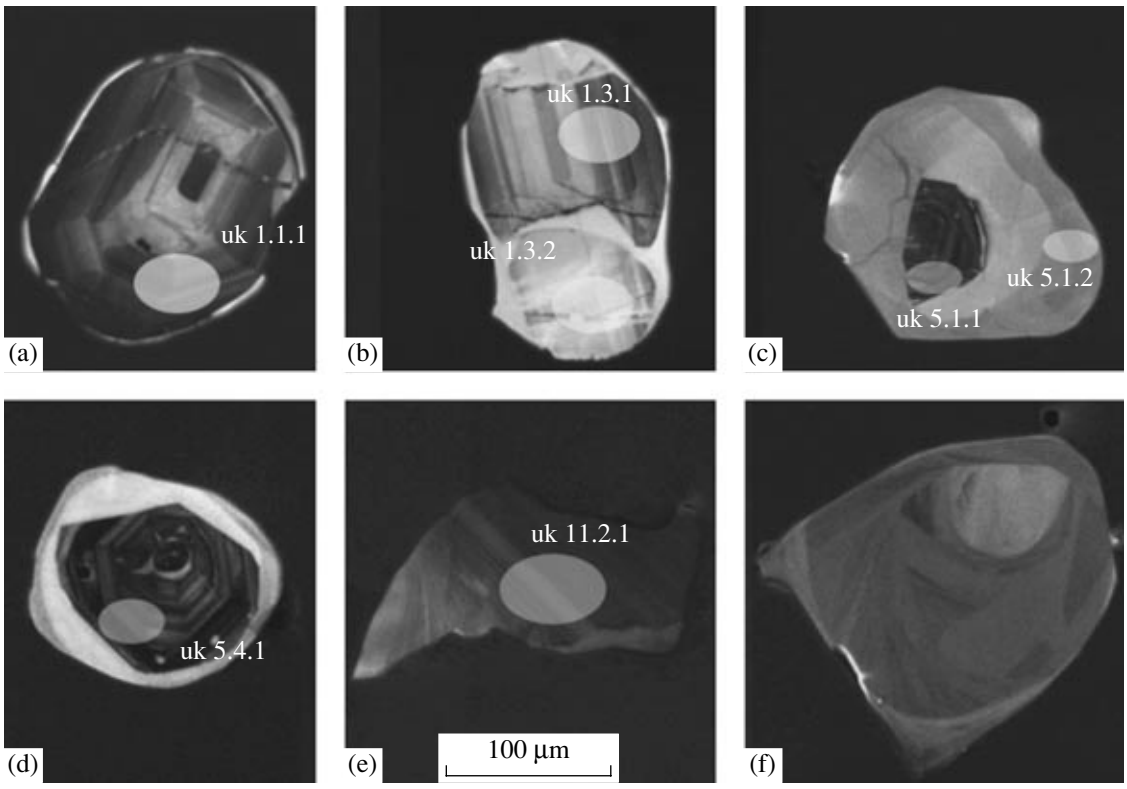

Fig. 1. Cathodoluminescence images of zircon grains. Ovals show analyzed area within grain.

uk11 and 1805 ± 43 Ma (MSWD = 2.8) for uk21. Zircon cores in xenoliths uk1 and uk5 define discordant values (Fig. 2a). Age values determined from $^{207}Pb/^{206}Pb$ are within 1770–3150 Ma.

Zircon cores from sample uk5 have wide variations of U and Th contents (table), averaging 309 and 157 ppm, respectively. The Th/U ratio varies in wide ranges. Rims have more steady composition: 31–36 ppm U, 7–9 ppm Th, and 0.21–0.24 Th/U. In sample uk1, cores also show wide variations in contents and ratios of these elements. The rim demonstrates the lowest Th/U ratio. Generally, the Th and U contents and their ratio are lower in the rims than in the cores.

We studied REE distribution in different zircon generations to decipher their origin. REE contents were determined on SHRIMP II at the Center of Isotopic Studies of Karpinskii All-Russia Institute. Cores in samples uk5 have similar REE abundance and distribution patterns (Fig. 3). The studied profiles exhibit a positive Ce anomaly (Ce/Ce* = 89–178), a negative Eu anomaly (Eu/Eu* = 0.31–0.54), and HREE depletion (Yb_N/Dy_N = 15–35). As compared to them, cores from sample uk1 are depleted in REE. They are characterized by less significant Ce and Eu anomalies (13 and 0.69, respectively) and strong HREE fractionation (Yb_N/Dy_N = 60), which is consistent with the mafic composition of this rock. Zircon rims in xenolith uk5 are distinguished from the cores by lower contents of REE, especially HREE (Yb_N/Dy_N = 10), and a lower Ce anomaly (49–74) (Fig. 3).

The rhythmic zoning and high Th/U ratio indicate a magmatic origin of zircon in the core. Despite the similarity in the internal structure of cores from one sample, the studied sample group could contain zircons crystallized from a parental melt (in the studied rock) and entrained from host rocks, because the Th and U contents in them show wide variations. However, cores of different ages from sample uk5 lack distinct differences in REE distribution patterns. This fact indicates their crystallization from a common melt. In sample uk1, sectors of cores crosscut by fractures are not displaced. Hence, zircon in rims and fractures is related to recrystallization of zircon in the core. One of the zircon fragments, which evidently belonged to a single crystal, is depleted in the Th and U content. This fragment is younger than another one (table, grain 3). In the cathodoluminescence image, rhythmic zoning in this fragment is vague (Fig. 1b). In this case, the age obtained does not correspond to the formation time, but reflects the loss of radiogenic Pb during the superimposed process. Thus, the protoliths of the studied xenoliths could have been formed in the Archean. This assumption is consistent with the model Sm–Nd age established in several similar xenoliths [5].

The formation of rims and rejuvenation of cores could be caused by granulite metamorphism. However,

U--Pb isotope data on zircons from xenolilths

Poin	Positio	$^{206}Pb_c$, %	U	Th	$^{232}Th/^{238}U$	$^{206}Pb^*$, ppm	Age, Ma		*D*, %	$^{207}Pb^*/^{206}Pb^*$	± %	$^{207}Pb^*/^{235}U$	± %	$^{206}Pb^*/^{238}U$	± %
			ppm				$^{206}Pb/^{238}U$	$^{207}Pb/^{206}Pb$							
uk5.1.1	Grain 1, c	0.02	175	105	0.62	48.5	1.805 ± 30	1.765 ± 33	−2	0.1080	1.8	4.81	2.6	0.3232	1.9
uk5.1.2	Grain 1, r	0.33	35	9	0.25	10.0	1.830 ± 37	1.835 ± 33	0	0.1121	1.8	5.08	3.0	0.3282	2.3
uk5.2.1	Grain 2, c	0.00	770	287	0.39	201	1.710 ± 83	1.877 ± 44	9	0.1148	2.4	4.81	6.0	0.3040	5.5
uk5.2.2	Grain 2, r	0.12	36	8	0.22	10.1	1.844 ± 30	1.800 ± 33	−2	0.1100	1.8	5.02	2.6	0.3312	1.9
uk5.3.1	Grain 3, c	0.09	263	177	0.69	70.9	1.756 ± 100	1.832 ± 38	4	0.1120	2.1	4.83	7.0	0.3130	6.7
uk5.3.3	Grain 3, r	0.03	33	7	0.23	9.63	1.882 ± 43	1.815 ± 44	−4	0.1110	2.4	5.19	3.6	0.3390	2.6
uk5.4.1	Grain 4, c	0.05	183	173	0.97	63.6	2.185 ± 110	2.709 ± 23	19	0.1862	1.4	10.36	6.1	0.4030	5.9
uk5.5.2	Grain 5, c	0.13	154	44	0.30	50.2	2.073 ± 97	2.245 ± 9.8	8	0.1415	0.57	7.40	5.5	0.3790	5.5
uk5.5.1	Grain 5, r	0.18	31	7	0.23	8.98	1.854 ± 31	1.819 ± 38	−2	0.1112	2.1	5.11	2.8	0.3332	1.9
uk1.1.1	Grain 1, c	0.07	239	103	0.44	109	2.732 ± 49	2.907 ± 180	6	0.2100	11	15.3	11.0	0.5280	2.2
uk1.2.1	Grain 2, r	0.69	31	2	0.08	8.92	1.835 ± 47	1.740 ± 45	−5	0.1065	2.4	4.83	3.8	0.3293	3.0
uk1.2.2	Grain 2, c	0.02	170	97	0.59	54.2	2.036 ± 30	2.008 ± 61	−1	0.1235	3.4	6.33	3.8	0.3715	1.7
uk1.3.1	Grain 3, c	0.03	83	27	0.33	27.9	2.133 ± 32	2.530 ± 82	16	0.1672	4.9	9.04	5.2	0.3922	1.7
uk1.3.2	Grain 3, c	0.14	28	15	0.55	7.54	1.747 ± 63	1.837 ± 31	5	0.1123	1.7	4.82	4.5	0.3110	4.1
uk1.4.1	Grain 4, c	0.01	210	54	0.27	58.4	1.805 ± 43	1.829 ± 20	1	0.1118	1.1	4.98	2.9	0.3231	2.7
uk1.5.1	Grain 5, c	0.00	118	57	0.50	43.7	2.309 ± 110	3.014 ± 71	23	0.2246	4.4	13.34	7.3	0.4310	5.8
uk1.6.1	Grain 6, c	0.01	85	40	0.49	39.0	2.771 ± 200	3.093 ± 95	10	0.2360	6.0	17.5	11.0	0.5370	9.0
uk1.6.2	Grain 6, c	0.00	37	8	0.28	18.9	2.996 ± 45	3.153 ± 11	5	0.2450	0.72	19.98	2.0	0.5920	1.9
uk21.2.1	Grain 2, c	0.03	559	95	0.18	151	1.762 ± 110	1.851 ± 33	5	0.1132	1.8	4.91	7.6	0.3140	7.3
uk21.1.1	Grain 1, r	0.63	17	5	0.28	4.71	1.763 ± 35	1.798 ± 51	2	0.1099	2.8	4.77	3.6	0.3146	2.3
uk11.2.1	Grain 2, c	0.01	315	323	1.06	87.2	1.801 ± 26	1.832 ± 8.6	2	0.1120	0.47	4.977	1.7	0.3222	1.6
uk11.1.1	Grain 1, r	0.01	154	122	0.82	42.0	1.781 ± 130	1.879 ± 35	5	0.1150	1.9	5.04	8.4	0.3180	8.1

Note: (c, r) core and rim, respectively; (*D*) Discordance; Confidence interval is 1σ. (Pb_c, Pb*) Common and radiogenic lead, respectively. Error in standard calibration was 0.66%. Common lead was corrected using measured ^{204}Pb.

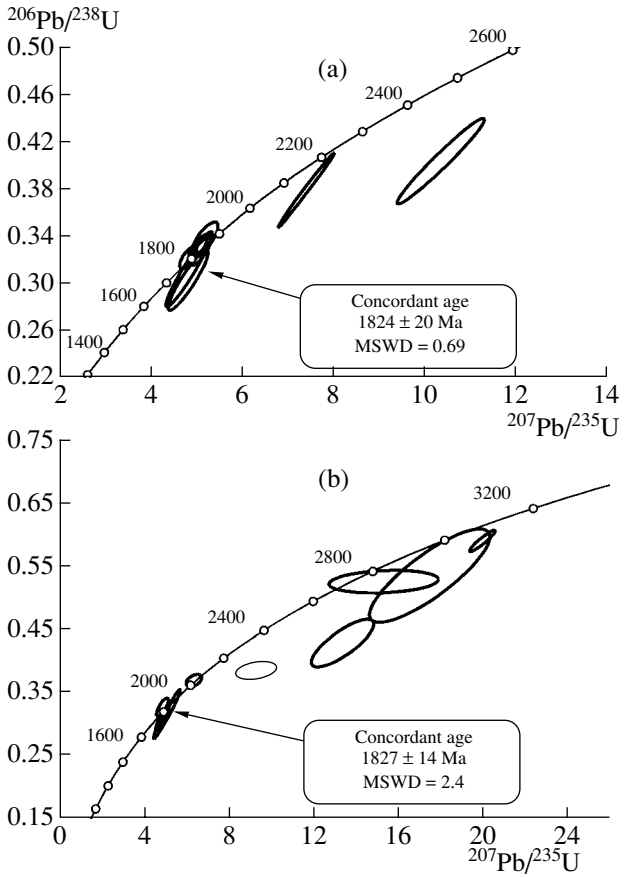

Fig. 2. Concordia diagram for zircons from xenoliths uk1 (a) and uk5 (b).

the Th/U ratio in the rims in most of the studied samples (except sample uk1) is higher than those typical of zircon from the granulite-facies rocks [13]. The significant HREE depletion of the rims (relative to the cores) is presumably caused by zircon growth in the presence of garnet, which also accumulates HREE. This phenomenon was observed in metamorphic rims and newly formed zircon grains from garnet granulites and eclogites [14].

The structure and composition of the cores indicate a primary magmatic origin of the zircon. Grain rims are equilibrated with garnet. Hence, they formed simultaneously with the mineral assemblage in the sample. Thus, their age (1.81–1.83 Ga) corresponds to the age of granulite metamorphism of the lower crustal rocks. The younger Grt–Cpx Sm–Nd age of granulite xenolith [1] reflects the closure of this system during cooling. The rims were formed by recrystallization of older zircon grains. The same process could be responsible for partial loss of radiogenic lead in the cores and rejuvenation of their age. However, the existence of entrained grains cannot be ruled out. In this case, the ancient datings reported in this paper indicate the Archean age of crustal rocks, which were intruded by parental melts. However, zircon cores from sample uk5 lack distinct

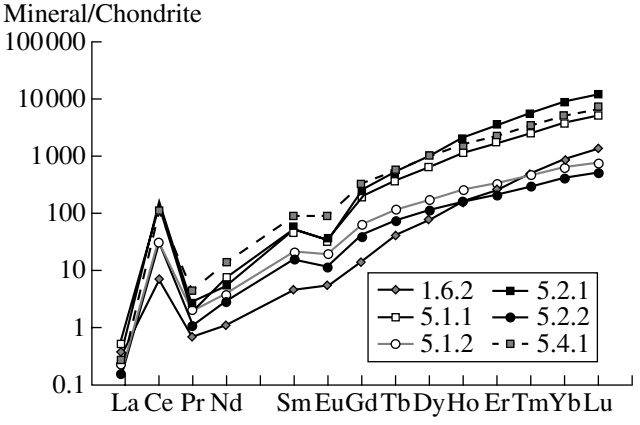

Fig. 3. Chondrite-normalized REE distribution patterns in zircons.

differences in REE patterns, indicating their crystallization from a common melt. Hence, it is possible that the protoliths of lower crustal granulites have an Archean age.

ACKNOWLEDGMENTS

This work was supported by the Russian Foundation for Basic Research, project nos. 02-05-64822 and 06-05-64416.

REFERENCES

1. L. A. Neimark, A. A. Nemchin, O. M. Rosen, et al., Dokl. Akad. Nauk **327**, 374 (1992).
2. O. M. Rose, V. P. Serenko, Z. V. Spetsius, et al., Geol. Geofiz. **43**, 3 (2002).
3. L. V. Solov'eva, B. M. Vladimirov, L. V. Dneprovskaya, et al., *Kimberlites and Kimberlite-Type Rocks: Upper Mantle Matter beneath Ancient Platforms* (Nauka, Novosibirsk, 1994) [in Russian].
4. L. V. Solov'eva, M. A. Gornova, M. E. Markova, and V. I. Lozhkin, Geochem. Int. **42**, 220 (2004) [Geokhimiya, No. 3, 270 (1994)].
5. V. P. Kovach, A. B. Kotov, A. P. Smelov, et al., Petrology **8**, 353 (2000) [Petrologiya **8**, 394 (2000)].
6. I. S. Williams, Rev. Econ. Geol. **7**, 1 (1998).
7. K. R. Ludwig, Berkley Geochronol. Center Spec. Publ., No. 2, 2000.
8. L. P. Black, S. L. Kamo, and I. S. Williams, Chem. Geol. **200**, 155 (2003).
9. Y. Ai, Contrib. Mineral. Petrol. **115**, 467 (1994).
10. E. J. Krogh-Ravna, J. Metamorph. Geol. **18**, 211 (2000).
11. R. C. Newton and D. Perkins III, Am. Mineral. **67**, 203 (1982).
12. L. P. Nikitina, in *Theophrastus Contributions to Advanced Studies in Geology. Capricious Earth: Models and Modeling of Geologic Processes and Objects* (St. Petersburg–Athens, 2000), Vol. 3.
13. P. W. O. Hoskin and U. Schaltegger, Rev. Miner. Geochem. **53**, 27 (2003).
14. D. Rubatto, Chem. Geol. **184**, 123 (2002).